and compound II at a retention time of 43 min. Another mutagen (compound III) was obtained from Fr. A-1-2 at a retention time of 33 min. Fr. A-2, dissolved in 45% tetrahydrofuran, was applied to the Luna 5 μ Phenyl-Hexyl column and eluted by the method used for Fr. A-1. Fractions with retention times of 26–28 min were evaporated to dryness. The residue was dissolved in 45% tetrahydrofuran and applied to the Inertsil ODS-EP column. By eluting with the gradient system used for Fr. A-1-1, a mutagen (compound IV) was isolated at a retention time of 39 min.

Fr. B was dissolved in 75% tetrahydrofuran and applied to the COSMOSIL $5C_{18}$ AR-II column. The materials were eluted with a gradient system of methanol in distilled water: 0–60 min, 87%; 60–70 min, a linear gradient of 87–100%; 70–90 min, 100%, at a flow rate of 3 ml/min. Aliquots of 3 ml were collected. Fractions with retention times of 34–37 min were evaporated and redissolved in 45% tetrahydrofuran to apply to the Luna 5 μ Phenyl-Hexyl column. Elution was performed with a gradient system of acetonitrile in distilled water: 0–60 min, 62%; 60–70 min, a linear gradient of 62–100%; 70–90 min, 100%, at a flow rate of 3 ml/min. Fractions with retention times of 42–44 min were evaporated. The residue, dissolved in 50% tetrahydrofuran, was applied to the Inertsil ODS-EP column and eluted with a gradient system of acetonitrile in distilled water: 0–60 min, 70%; 60–70 min, a linear gradient of 70–100%; 70–90 min, 100%, at a flow rate of 0.7 ml/min. A mutagen (compound V) was isolated at a retention time of 50 min.

All HPLC procedures were carried out at 30 C, and the eluates were monitored for UV absorption at 254 nm using an SPD M10Avp diode array detector (Shimadzu Co., Kyoto, Japan). An aliquot of each fraction of the eluate was used for mutagenicity assay.

2.4. HPLC analysis of nitroarenes

Authentic 1,6-DNP, 1,8-DNP, 3,6-DNBeP, 3,9-DNF, and 1,3,6-TNP were dissolved in ethanol and analyzed by HPLC. Each sample was injected into the Inertosil ODS-EP column and eluted with the following solution: 60% acetonitrile for 1,6-DNP, 1,8-DNP, 3,9-DNF, and 1,3,6-TNP; 70% acetonitrile for 3,6-DNBeP. These five standards were also applied to the Luna 5 μ Phenyl-Hexyl column and eluted under the following conditions: 60% acetonitrile for 1,6-DNP, 1,8-DNP, 3,9-DNF, and 1,3,6-TNP; 62% acetonitrile for 3,6-DNBeP. All HPLC procedures were performed at 30 °C. Elution was conducted at a flow rate of 0.7 ml/min. Eluents were monitored with the Shimadzu SPD-M10Avp diode array detector.

2.5. Spectral measurement

UV absorption spectra were measured with the Shimadzu LC-VP HPLC system using an SPD M10Avp diode array detector. Electron impact mass spectra (EI-MS) were measured at 70 eV using a Shimadzu QP5050A mass spectrometer with a direct inlet system.

2.6. Mutagenicity test

All of the samples were dissolved in dimethyl sulfoxide and assayed for mutagenicity by the preincubation method [35] using *Salmonella typhimurium* TA98 and TA100 [36]. The S9 mix contained 0.05 ml of S9, prepared from livers of male Sprague-Dawley rats treated with phenobarbital and β-naphthoflavone, in a total volume of 0.5 ml. The mutagenic potencies of samples were calculated from linear portions of the dose–response curves, which were obtained with three or four doses and duplicate plates at each dose. The slope of the dose–response curve was adapted as the mutagenic potency. When the samples induced twofold increases over the average yield of spontaneous revertants and showed well-behaved concentration-response patterns, the samples were judged positive.

2.7. Detection of mutagens in surface soils from Aichi prefecture (Hekinan and Nagoya) and Osaka prefecture (Izumiotsu and Takatsuki)

Organic extracts from surface soil samples collected in Hekinan in January 2001, Nagoya in January 2001, and Izumiotsu in February 2002 were also prepared by Soxhlet extraction [32]. In addition, soil sample was collected in Takatsuki in January 2003, and the organic extract (3.0 g) was prepared from sieved soil (3.6 kg). These four Soxhlet extracts were successively fractionated with the Sephadex LH-20, silica gel, and the Ultra pack ODS columns as described for the sample from Kyoto. An aliquot of each fraction was examined for mutagenicity. Mutagenic fractions from the four samples, which corresponded to Fr. A for the sample from Kyoto, were evaporated to dryness. For the sample from Takatsuki, a fraction corresponding to Fr. B of the sample from Kyoto was also obtained. The residues were further separated by the same fractionation methods, using the COSMOSIL $5C_{18}$ AR-II, the Luna 5 μ Phenyl-Hexyl, and Inertsil ODS-EP columns, as described for the sample from Kyoto.

3. Results

3.1. Mutagenicity of surface soil in Kyoto

Surface soil samples were collected from 11 sites in Kyoto city and one site in its neighboring city, Mukomachi. Fig. 1 shows the location of sampling sites. At each site, soil samples were collected twice or three times between December 2003 and January 2006. Table 1 summarizes the mutagenicity of the soil samples toward *S. typhimurium* TA98 and TA100. Almost all, i.e. 23/25 (92%) and 24/25 (96%), samples showed mutagenicity in TA98 without and with S9 mix, respectively. On the other hand, 14/25 (56%) and 18/25 (72%) of the samples were positive in TA100 without and with S9 mix, respectively. Six (24%) and two (8%) sam-

Table 1
Mutagenicities of organic extracts from surface soil collected in Kyoto and Mukomachi cities

Site No.	Sampling site	Sampling date	Mutagenicity (revertants/g of soil)[a]			
			TA98		TA100	
			−S9 mix	+S9 mix	−S9 mix	+S9 mix
Kyoto city						
1	Sakyo Ward	December 2004	3780	4930	395	801
		January 2006	ND[b]	53	ND	ND
2	Kamigyo Ward	December 2003	995	675	142	276
		December 2004	ND	ND	ND	ND
3	Ukyo Ward 1	December 2003	833	407	88	250
		December 2004	796	791	78	432
4	Nakagyo Ward 1	December 2003	10,060	857	700	843
		December 2004	157	47	ND	156
5	Nakagyo Ward 2	December 2003	3087	2237	299	616
		December 2004	102	48	ND	ND
6	Ukyo Ward 2	December 2003	833	407	88	250
		December 2004	796	791	78	432
7	Shimogyo Ward 1	December 2003	448	636	122	695
		December 2004	96	39	ND	ND
8	Shimogyo Ward 2	December 2003	245	155	ND	199
		December 2004	288	83	ND	ND
9	Minami Ward 1	December 2004	2904	3546	360	1082
		April 2005	5329	5363	1013	1999
		January 2006	12,870	4264	2316	2,620
10	Fushimi Ward	December 2003	4893	1612	601	1759
		December 2004	143	67	ND	ND
11	Minami Ward 2	December 2003	3184	1707	441	893
		December 2004	191	51	ND	ND
12	Mukomachi city	December 2003	204	141	ND	345
		December 2004	83	93	ND	82

[a] Organic extracts were obtained from 15 g of soil (<250 mm) with an ultrasonic extractor. The slope (revertants/g of soil) of the dose–response curve was calculated by least-squares linear regression from the first linear portion of the dose–response curve.
[b] ND = not detected.

ples showed high (1000–10,000 revertants/g of soil) and extreme (more than 10,000 revertants/g of soil) mutagenicity, respectively, in TA98 without and/or with S9 mix. For TA100, four samples (16%) were highly mutagenic without and/or with S9 mix, but no sample was extreme. Soil samples were collected three times at site No. 9 (Minami Ward 1) and all samples showed high or extreme mutagenicity in TA98 and TA100. Other five samples, which showed high or extreme mutagenicity in TA98 and/or TA100, were collected from five sites. The highest mutagenic potency was detected for the sample collected at site No. 9 in January 2006, and the extracts induced 12,870 revertants in TA98 per gram of soil equivalent without S9 mix.

3.2. *Isolation and identification of mutagens in surface soil in Kyoto*

To identify the major mutagens in surface soil, organic extract was prepared from the soil samples collected at site No. 9. This soil extract, which showed potent mutagenicity in TA98 without S9 mix (13,640 revertants/mg of extract), was fractionated by diverse column chromatography methods by monitoring the mutagenicity of the fractions in TA98 without S9 mix. First, the soil extract was applied to a Sephadex LH-20 column. Mutagenicity was detected in several fractions, and the most potent mutagenicity was observed in the fraction with elution volumes of 210–330 ml. This mutagenic frac-

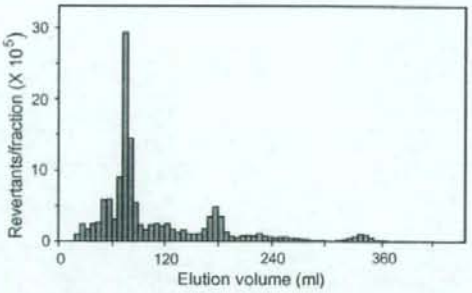

Fig. 2. LPLC profile of mutagens in the sample collected at site No. 9, Minami Ward 1, in Kyoto. LPLC was performed on an Ultra pack ODS column. The mutagenicity of each 6 ml fraction was assayed in *S. typhimurium* TA98 without S9 mix.

tion was separated by LPLC using a silica gel column, and fractions with potent mutagenicity were obtained at elution volumes of 540–795 ml. Mutagenicity of these highly active fractions eluted from the silica gel column corresponded to 71% of the total mutagenicity of the soil extract. This fraction was applied to an Ultra pack ODS column for LPLC. Fig. 2 shows the mutagenicity profile of the eluate. Many fractions showed mutagenicity, and high potencies were detected in fractions with elution volumes of 18–96 ml and 156–198 ml. These two fractions were designated as Fr. A and Fr. B, respectively. The contribution ratios of Fr. A and Fr. B to the total mutagenicity of the soil extract were 48 and 9%, respectively.

Fr. A was further separated by HPLC using a COSMOSIL $5C_{18}$ AR-II column. Potent mutagenicity was observed in fractions with retention times of 33–37 and 44–48 min, which were designated as Fr. A-1 and Fr. A-2, respectively. Fr. A-1 was further separated on a Luna 5 μ Phenyl-Hexyl column, and two highly mutagenic fractions were obtained at retention times of 27–29 and 36–38 min. These two mutagenic fractions, designated as Fr. A-1-1 and Fr. A-1-2, respectively, were separated on an Inertsil ODS-EP column. For Fr. A-1-1, UV absorption peaks, which showed potent mutagenicity, were observed at retention times of 40 and 43 min, and these peak fractions were designated as compound I and compound II, respectively (Fig. 3(a)). In a similar way, another UV absorption peak fraction (compound III), which showed strong mutagenicity, was isolated from Fr. A-1-2 at a retention time of 33 min, as shown in Fig. 4(a). Fr. A-2 was also separated by HPLC on the Luna 5 μ Phenyl-Hexyl column. A highly mutagenic fraction was obtained at retention times of 26–28 min, and this mutagenic fraction was further separated on the

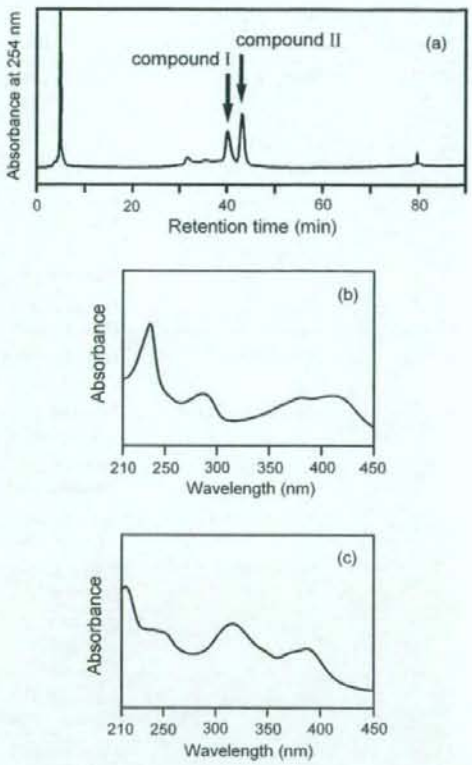

Fig. 3. HPLC profile (a) and UV absorption spectra (b and c) of compounds I and II isolated from surface soil from site No. 9, Minami Ward 1, in Kyoto. HPLC was performed on an Inertsil ODS-EP column, and eluted with the following gradient system of acetonitrile in distilled water: 0–60 min, 60%; 60–70 min, linear gradient of 60–100%; 70–90 min, 100%, at a flow rate of 0.7 ml/min. UV absorption peaks corresponding to compounds I and II are indicated by arrows in the HPLC profile (a). UV absorption spectra of compounds I and II are shown in (b) and (c), respectively.

Inertsil ODS-EP column. As shown in Fig. 5(a), a UV absorption peak, which showed strong mutagenicity, was observed at retention times of 39 min, and this mutagen was designated as compound IV.

Fr. B was applied to the COSMOSIL $5C_{18}$ AR-II column, and potent mutagenicity was observed in the fraction with retention times of 34–37 min. This mutagenic fraction was further separated on the Luna 5 μ Phenyl-Hexyl column. Resulting fractions with retention times of 42–44 min, which showed potent mutagenicity, was further applied to the Inertsil ODS-EP column, and a mutagen (compound V) was isolated as a UV absorption peak at a retention time of 50 min (Fig. 6(a)). Contribu-

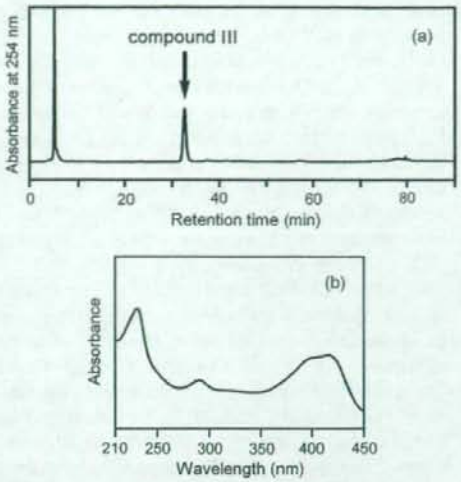

Fig. 4. HPLC profile (a) and UV absorption spectrum (b) of compound III isolated from surface soil from site No. 9, Minami Ward 1, in Kyoto. HPLC was performed on an Inertsil ODS-EP column, and eluted with the following gradient system of acetonitrile in distilled water: 0–60 min, 60%; 60–70 min, linear gradient of 60–100%; 70–90 min, 100%, at a flow rate of 0.7 ml/min. UV absorption peak corresponding to compound III is indicated by an arrow in the HPLC profile (a).

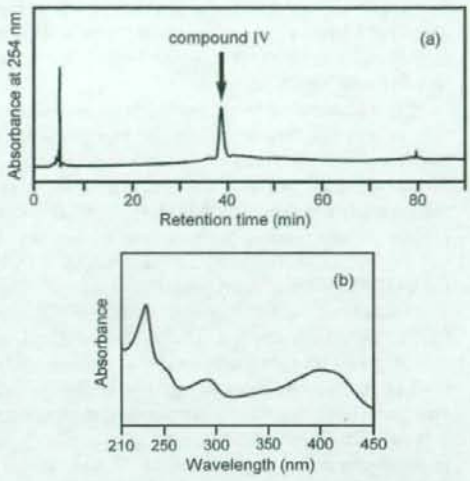

Fig. 5. HPLC profile (a) and UV absorption spectrum (b) of compound IV isolated from surface soil from site No. 9, Minami Ward 1, in Kyoto. HPLC was performed on an Inertsil ODS-EP column, and eluted with the following gradient system of acetonitrile in distilled water: 0–60 min, 60%; 60–70 min, linear gradient of 60–100%; 70–90 min, 100%, at a flow rate of 0.7 ml/min. UV absorption peak corresponding to compound IV is indicated by an arrow in the HPLC profile (a).

tion ratios of compounds I–V to the total mutagenicity of soil extracts in TA98 without S9 mix were 3, 10, 10, 10, and 6%, respectively.

3.3. Identification of compounds I–V

UV absorption spectra of compounds I, IV, and V, which are shown in Figs. 3(b), 5(b), and 6(b), were consistent with those of 1,6-DNP, 1,8-DNP, and 3,6-DNBeP, respectively. Retention times of compounds I, IV, and V on the Inertsil ODS-EP column were found to be the same as those of 1,6-DNP, 1,8-DNP, and 3,6-DNBeP, respectively. Moreover, retention times of 1,6-DNP, 1,8-DNP, and 3,6-DNBeP on the Luna 5 μ Phenyl-Hexyl column were 28, 27, and 43 min, respectively. These retention times corresponded to those of mutagenic fractions from with compounds I, IV, and V were isolated. As shown in Fig. 7, molecular ion peaks of compounds II and III were observed at *m/z* 292 and 337, respectively. Mass spectra of compounds II and III were consistent with those of authentic 3,9-DNF and 1,3,6-TNP. UV absorption spectra of compounds II and III, which are shown in Figs. 3(c) and 4(b), were consistent with those of 3,9-DNF and 1,3,6-TNP, respectively. Retention times of compounds II and III on the Inertsil ODS-EP column and the Luna 5 μ Phenyl-Hexyl column were found to coincid with those of 3,9-DNF and 1,3,6-TNP, respectively. On the basis of these results, compounds I–V were concluded to be 1,6-DNP, 3,9-DNF, 1,3,6-TNP, 1,8-DNP, and 3,6-DNBeP, respectively. The chemical structures of these nitroarenes are shown in Fig. 8.

3.4. Detection of nitroarenes in surface soil collected in other prefectures

To investigate the distribution of 1,6-DNP, 1,8-DNP, 3,9-DNF, 1,3,6-TNP, and 3,6-DNBeP in surface soil in other residential areas, organic extracts of soil samples collected in different four cities were examined. In a previous study [32], we analyzed soil samples collected in Izumiotsu, Hekinan, and Nagoya between January 2001 and February 2002, which showed potent mutagenicity in TA98 without S9 mix (1240–14,460 revertants/mg of extract), and 3,6-DNBeP was detected from all soil samples. These three soil samples were examined for 1,6-DNP, 1,8-DNP, 3,9-DNF, and 1,3,6-TNP in this study. The organic extract of a surface soil sample collected in Takatsuki in January 2003 showed strong mutagenicity toward TA98 without S9 mix (337,800 revertants/mg of extract) and was also examined for all

five nitroarenes in this study. These four soil extracts were fractionated by the method used for the soil sample from Kyoto, monitoring the mutagenicity of the fractions in TA98 without S9 mix.

Potent mutagenicity was detected in the fractions with elution volumes similar to those of highly mutagenic fractions for the sample from Kyoto on Sephadex LH-20 and silica gel columns. These active fractions were subsequently separated with the Ultra pack ODS column. Fractions corresponding to Fr. A from all soil samples and Fr. B from the sample from Takatsuki on the Ultra pack ODS column showed potent mutagenicity. These active fractions were further separated by HPLC using COSMOSIL $5C_{18}$ AR-II, Luna 5 μ Phenyl-Hexyl, and then Inertsil ODS-EP columns under the same conditions used for the sample from Kyoto. Potent mutagenicity was found in the fractions corresponding to compounds I–IV in each fractionation step for all samples. Mutagens corresponding to compounds I–IV were eluted at retention times of 40, 43, 33, and 39 min, respectively, as single UV absorption peaks on the Inertsil ODS-EP column. The retention times and UV absorption spectra of these peak fractions coincided with those of 1,6-DNP, 3,9-DNF, 1,3,6-TNP, and 1,8-DNP, respectively. On the basis of these results, the mutagens corresponding to compounds I–IV isolated from soil samples from four cities other than Kyoto were concluded to be 1,6-DNP, 3,9-DNF, 1,3,6-TNP, and 1,8-DNP, respectively. A mutagen corresponding to compound V was isolated from Fr. B prepared from the sample from Takatsuki and was deduced to be 3,6-DNBeP by consistency of the retention time on HPLC using the Luna 5 μ Phenyl-Hexyl and the Inertsil ODS-EP columns and UV absorption spectrum of the mutagen and those of the authentic compound.

The amounts of 1,6-DNP, 1,8-DNP, 3,9-DNF, 1,3,6-TNP, and 3,6-DNBeP in soil extracts from soil samples and their percent contributions to the total mutagenicity of the extracts are shown in Table 2. The amounts of nitroarenes were from 0.14 to 66.26 ng/mg of extract. The highest levels of nitroarenes were detected in the soil sample collected in Takatsuki. Percent contributions of each nitroarene ranged from 0.7 to 22%. For the soil sample from site No. 9 in Kyoto, percent contributions of 1,3,6-TNP, and 3,9-DNF were relatively high, and the values were the same as that of 1,8-DNP, i.e. 10%. In contrast, for the soil sample from Takatsuki, the percent contribution of 1,8-DNP was particularly high, i.e.

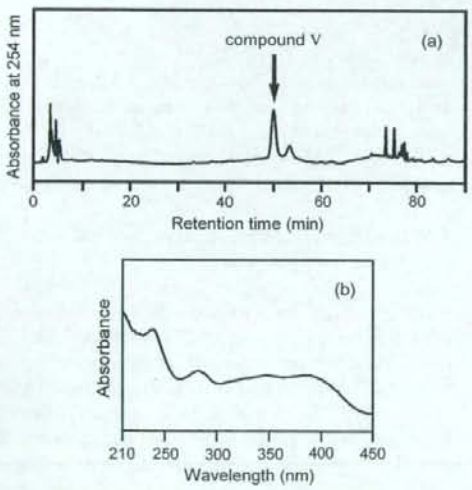

Fig. 6. HPLC profile (a) and UV absorption spectrum (b) of compound V isolated from surface soil from site No. 9, Minami Ward 1, in Kyoto. HPLC was performed on an Inertsil ODS-EP column, and eluted with the following gradient system of acetonitrile in distilled water: 0–60 min, 60%; 60–70 min, linear gradient of 60–100%; 70–90 min, 100%, at a flow rate of 0.7 ml/min. UV absorption peak corresponding to compound V is indicated by an arrow in the HPLC profile (a).

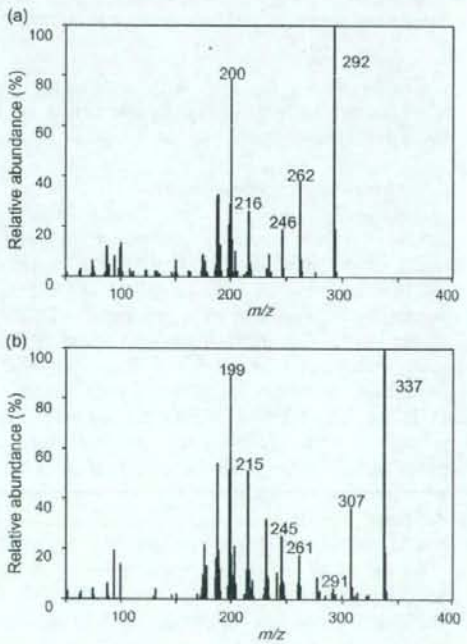

Fig. 7. Electron impact mass spectra of compounds II and III isolated from surface soil from site No. 9, Minami Ward 1, in Kyoto.

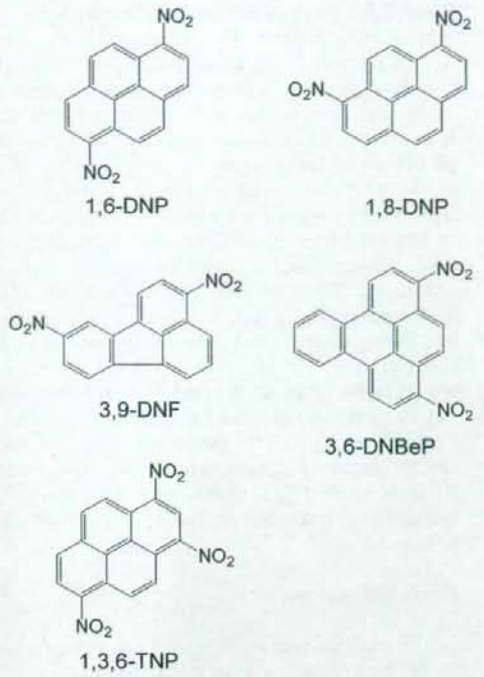

Fig. 8. Chemical structures of 1,6- and 1,8-dinitropyrene (DNP) isomers, 3,9-dinitrofluoranthene (DNF), 1,3,6-trinitropyrene (TNP), and 3,6-dinitrobenzenzo[*e*]pyrene (DNBeP).

22%, and that of 1,3,6-TNP was the lowest, i.e. 0.7%, among the soil samples examined. For the sample from Izumiotsu, the contribution of 1,3,6-TNP was relatively low. The total percent contributions of five nitroarenes to these five soil extracts were from 39 to 45%.

4. Discussion

In a previous study [28], we examined the mutagenicity of 544 surface soil samples collected in five geographically different regions of Japan, i.e. Hokkaido, Kanto, Chubu, Kinki, and Kyushu regions, by the Ames assay using *S. typhimurium* TA98 and TA100 with and without S9 mix. On the basis of mutagenic potency, these soil samples were classified into four levels, i.e. low (up to 100 revertants/g of soil), moderate (100–1000 revertants/g of soil), high (1000–10,000 revertants/g of soil), and extreme (more than 10,000 revertants/g of soil). The percentage of soil samples classified as high ($n = 86$) and extreme ($n = 8$) were 16 and 1.5%, respectively. In this study, sample

Table 2
Amounts of nitroarenes and their contribution ratios of nitroarenes to the mutagenicities of organic extracts from surface soil in *S. typhimurium* TA98 without S9 mix

Sampling site	Mutagenicity (revertants/mg of extract)	Amount (ng/mg of extract)					Contribution ratio (%)					Total
		1,6-DNP	1,8-DNP	1,3,6-TNP	3,9-DNF	3,6-DNBeP	1,6-DNP	1,8-DNP	1,3,6-TNP	3,9-DNF	3,6-DNBeP	
Kyoto prefecture												
Kyoto (site No. 9)	13,640	0.89	1.75	12.29	3.81	0.93	3	10	10	10	6	39
Aichi prefecture												
Nagoya	14,460[a]	1.19	1.33	10.29	3.48	2.72	4	7	8	9	16[a]	44
Hekinan	1,240[a]	0.14	0.14	0.96	0.22	0.31	5	9	4	6	21[a]	45
Osaka prefecture												
Izumiotsu	5,280[a]	0.35	0.73	1.02	1.48	1.08	3	11	2	10	17[a]	43
Takatsuki	337,800	34.46	66.26	15.04	23.30	29.79	6	22	0.7	4	11	43.7

DNP, dinitropyrene; TNP, trinitropyrene; DNF, dinitrofluoranthene; NBeP, dinitrobenzo[*e*]pyrene.
[a] From Ref. [32].

collection was performed twice or three times at 12 sites, and 25 surface soil samples were collected. Almost all samples showed mutagenicity in TA98 with and without S9 mix, and eight (32%) samples showed high or extreme mutagenicity. Three soil samples collected at site No. 9 (Minami Ward 1) showed high or extreme mutagenicity in TA98, and the other highly or extremely mutagenic soil samples were collected at five sites. These results suggest that surface soil was extensively contaminated with mutagens in the residential area in Kyoto, and there were some sites where contamination levels were high. The pollution of surface soil at site No. 9 was thought to be severe and persistent.

As major mutagenic constituents, five compounds were isolated from surface soil samples from site No. 9, and were identified to be 1,6-DNP, 1,8-DNP, 1,3,6-TNP, 3,9-DNF, and 3,6-DNBeP. Many researchers have reported the biological activity, including carcinogenicity, of these nitroarenes, which are highly mutagenic in TA98 without S9 mix; inducing 175,000 revertants/nmol of 1,6-DNP [29], 257,000 revertants/nmol of 1,8-DNP [29], 65,500 revertants/nmol of 1,3,6-TNP [34], 104,000 revertants/nmol of 3,9-DNF [33], and 285,000 revertants/nmol of 3,6-DNBeP [32]. 1,6-DNP, 1,8-DNP and 1,3,6-TNP showed mutagenicity at the hypoxanthine–guanine phosphoribosyl transferase gene locus in cultured Chinese hamster ovary cells [37] and were mutagenic in Chinese hamster lung (CHL) cells for the induction of diphtheria toxin resistance [38]. 3,9-DNF induced chromosomal aberration in CHL cells [39]. 1,6-DNP, 1,8-DNP and 3,9-DNF showed carcinogenicity in experimental animals [30,31,40] and are classified as possible human carcinogens (group 2B) by the International Agency for Research on Cancer (IARC) [9,41]. 3,6-DNBeP is a novel chemical and was newly detected as a major mutagenic constituent in surface soil [32]. Except for mutagenicity in *S. typhimurium* strains, no other biological activity of 3,6-DNBeP has been reported. As 3,6-DNBeP is an extremely potent bacterial mutagen, other biological activities of 3,6-DNBeP, including carcinogenicity, should be elucidated.

All five nitroarenes identified as major mutagenic constituents in surface soil from Kyoto were found in other highly mutagenic soil samples collected in Aichi and Osaka prefectures. The amounts of the five nitroarenes ranged from 0.14 to 66.26 ng/mg of extract. The percent contributions of these nitroarenes to the total mutagenicity of soil extracts were from 0.7 to 22%. The amounts and percent contributions of these nitroarenes were comparable to those of 1,6- and 1,8-DNP isomers detected in soil samples from the Kinki Region [25]. The total percent contributions of the five nitroarenes to these five soil extracts were from 39 to 45% in this study. The results suggest that these five nitroarenes might be major mutagenic constituents of the surface soil in the five residential areas investigated in this study. Relative contribution ratios of the five nitroarenes to the mutagenicity of the five soil samples were different among soil samples. Nitroarenes are formed by incomplete combustion of organic matter, such as fossil fuels. The differences of the relative contributions of nitroarenes among soil samples might be attributed to the combustion conditions, which affect the formation of incomplete combustion products, such as different fuels and combustion temperatures at the sources of the nitroarenes. To clarify the sources, the quantification of these nitroarenes in airborne particles over extensive areas and in exhaust particles from potential origins such as the engines of motor vehicles, incinerators, and furnaces is required. The exposure levels of inhabitants to theses nitroarenes should be assessed to estimate their impact on human health and biota.

Conflict of interest

This study has been performed for academic purposes neither for companies producing chemicals that were used and/or mentioned in this study nor for the competing companies. I do not receive direct or indirect rewards from any source for writing this manuscript.

Acknowledgements

This study was partially supported by Grants-in-Aid for Cancer Research from the Ministry of Health and Welfare of Japan and Scientific Research from the Ministry of Education, Culture, Sports, Science and Technology of Japan, and funds under a contract with the Ministry of the Environment of Japan.

References

[1] A. Höner, M. Arnold, N. Hüsers, W. Kleiböhmer, Monitoring polycyclic aromatic hydrocarbons in waste gases, J. Chromatogr. A 710 (1995) 129–137.
[2] A. Pinter, K. Bejczi, M. Csik, Z. Kelecsenyi, M. Kertesz, A. Surjan, G. Torok, Mutagenicity of emission and immission samples around industrial areas, IARC Sci. Publ. 104 (1990) 269–276.
[3] M. Ayras, H. Niskavaara, I. Bogatyrev, V. Chekushin, V. Pavlov, P. de Caritat, J.H. Halleraker, T.E. Finne, G. Kashulina, C. Reimann, Regional patterns of heavy metals (Co, Cr, Cu, Fe, Ni, Pb, V and Zn) and sulfur in terrestrial moss samples as indication of airborne pollution in a 188,000 km^2 area in northern Finland, Norway and Russia, J. Geochem. Explor. 58 (1997) 269–281.

[4] M. Ragosta, R. Caggiano, M. D'Emilio, M. Macchiato, Source origin and parameters influencing levels of heavy metals in TSP, in an industrial background area of Southern Italy, Atmos. Environ. 36 (2002) 3071–3087.
[5] A. Kamiya, Y. Ose, Isolation of dinitropyrene in emission gas from a municipal incinerator and its formation by a photochemical reaction, Sci. Total Environ. 72 (1988) 1–9.
[6] T.R. Henderson, J.D. Sun, R.E. Royer, C.R. Clark, A.P. Li, T.M. Harvey, D.H. Hunt, J.E. Fulford, A.M. Lovette, W.R. Davidson, Triple-quadrupole mass spectrometry studies of nitroaromatic emissions from different diesel engines, Environ. Sci. Technol. 17 (1983) 443–449.
[7] T. Handa, T. Yamauchi, K. Sawai, T. Yamamura, Y. Koseki, T. Ishii, In situ emission levels of carcinogenic and mutagenic compounds from diesel and gasoline engine vehicles on an expressway, Environ. Sci. Technol. 18 (1984) 895–902.
[8] A.J. Cohen, Outdoor air pollution and lung cancer, Environ. Health Perspect. 47 (Suppl. 4) (2000) 115–140.
[9] IARC, IARC Monographs on the evaluation of carcinogenic risks to humans, vol. 46: Diesel and gasoline engine exhausts and some nitroarenes, International Agency for Research on Cancer, Lyons, France, 1989.
[10] V.E. Archer, Air pollution and fatal lung disease in three Utah counties, Arch. Environ. Health 45 (1990) 325–334.
[11] D.W. Dockery, C.A. Pope III, X. Xu, J.D. Spengler, J.H. Ware, M.E. Fay, B.G. Ferris Jr., F.E. Speizer, An association between air pollution and mortality in six U.S. cities, N. Engl. J. Med. 329 (1993) 1753–1759.
[12] C.A. Pope III, M.J. Thun, M.M. Namboodiri, D.W. Dockery, J.S. Evans, F.E. Speizer, C.W. Heath Jr., Particulate air pollution as a predictor of mortality in a prospective study of U.S. adults, Am. J. Respir. Crit. Care Med. 151 (1995) 669–674.
[13] F. Barbone, M. Bovenzi, F. Cavalleri, G. Stanta, Air pollution and lung cancer in Trieste, Italy, Am. J. Epidemiol. 141 (1995) 1161–1169.
[14] IARC, IARC Monographs on the evaluation of carcinogenic risks to humans, vol. 34: Polynuclear aromatic compounds. Part 3. Industrial exposures in aluminium production, coal gasification, coke production, and iron and steel founding, International Agency for Research on Cancer, Lyons, France, 1984.
[15] O.L. Lloyd, G. Smith, M.M. Lloyd, Y. Holland, F. Gailey, Raised mortality from lung cancer and high sex ratios of births associated with industrial pollution, Brit. J. Ind. Med. 42 (1985) 475–480.
[16] K. Arashidani, T. Someya, M. Yoshikawa, Y. Kodama, Polynuclear aromatic hydrocarbon concentration and mutagenic activity in soils sampled at the roadsides, J. Jpn. Soc. Air Pollut. 27 (1992) 190–197.
[17] K. Tamakawa, Y. Takahashi, Y. Mishima, T. Seki, A. Tsunoda, Mutagenicity and benzo[*a*]pyrene contents in soils in Sendai City. Influence of particulate substances produced by studded tires of automobiles, Eisei Kagaku 31 (1985) 329–333.
[18] H.F. Wesp, X. Tang, R. Edenharder, The influence of automobile exhausts on mutagenicity of soils: contamination with, fractionation, separation, and preliminary identification of mutagens in the *Salmonella*/reversion assay and effects of solvent fractions on the sister-chromatid exchanges in human lymphocyte cultures and in the in vivo mouse bone marrow micronucleus, Mutat. Res. 472 (2000) 1–21.
[19] T. Watanabe, K.R. Wannee, M. Asanoma, A. Tepsuwan, N. Tantasri, N. Meesiripan, T. Hasei, T. Hirayama, K. Wakabayashi, Mutagenicity of surface soils in urban areas of Aichi prefecture, Japan, and Bangkok, Thailand, J. Health Sci. 51 (2005) 645–657.
[20] T. Nishimura, S. Goto, Y. Kata, M. Okunuki, H. Matsushita, Mutagenicity and benzo[*a*]pyrene contents in soils in Tokyo, J. Jpn. Soc. Air Pollut. 19 (1984) 228–238.
[21] W. Goggleman, P. Spitzauer, Mutagenic activity in agricultural soils, in: H. Stich (Ed.), Carcinogens and Mutagens in the Environment, vol. 3, CRC Press, Orlando, FL, 1982, pp. 178–183.
[22] K.W. Brown, K.C. Donnelly, J.C. Thomas, P. Davol, B.R. Scott, Mutagenicity of three agricultural soils, Sci. Total Environ. 41 (1985) 173–186.
[23] R. Edenharder, M. Ortseifen, M. Koch, H.F. Wesp, Soil mutagens are airborne mutagens: variation of mutagenic activities induced in *Salmonella typhimurium* TA98 and TA100 by organic extracts of agricultural and forest soils in dependence on location and season, Mutat. Res. 472 (2000) 23–36.
[24] M.G. Knize, B.T. Takemoto, P.R. Lewis, J.S. Felton, The characterization of the mutagenic activity of soil, Mutat. Res. 192 (1987) 23–30.
[25] T. Watanabe, T. Hasei, Y. Takahashi, S. Otake, T. Murahashi, T. Takamura, T. Hirayama, K. Wakabayashi, Mutagenic activity and quantification of nitroarenes in surface soil in the Kinki region of Japan, Mutat. Res. 538 (2003) 121–131.
[26] P.A. White, L.D. Claxton, Mutagens in contaminated soil: a review, Mutat. Res. 567 (2004) 227–345.
[27] T. Watanabe, S. Goto, Y. Matsumoto, M. Asanoma, T. Hirayama, N. Sera, Y. Takahashi, O. Endo, S. Sakai, K. Wakabayashi, Mutagenic activity of surface soil and quantification of 1,3-, 1,6-, and 1,8-dinitropyrene isomers in soil in Japan, Chem. Res. Toxicol. 13 (2000) 281–286.
[28] O. Endo, S. Goto, Y. Matsumoto, S. Sakai, T. Akutagawa, M. Asanoma, T. Hirayama, T. Watanabe, H. Tsukatani, N. Sera, A. Tada, K. Wakabayashi, Mutagenicity of airborne particles, river waters and soils in Japan from 1996 to 2003, Environ. Mutagen Res. 26 (2004) 9–22.
[29] H. Tokiwa, Y. Onishi, Mutagenicity and carcinogenicity of nitroarenes and their sources in the environment, CRC Crit. Rev. Toxicol. 17 (1986) 23–60.
[30] P.G. Wisloki, E.S. Bagan, A.Y.H. Lu, K.L. Dooley, P.P. Fu, H. Han-Hsu, F.A. Beland, F.F. Kadlubar, Tumorigenicity of nitrated derivatives of pyrene, banz[*a*]anthracene, chrysene and benzo[*a*]pyrene in the newborn mouse assay, Carcinogenesis 7 (1986) 1317–1322.
[31] K. Imaida, M. Lee, S.J. Land, C.Y. Wang, C.M. King, Carcinogenicity of nitropyrenes in the newborn female rat, Carcinogenesis 16 (1995) 3027–3030.
[32] T. Watanabe, T. Hasei, T. Takahashi, M. Asanama, T. Murahashi, T. Hirayama, K. Wakabayashi, Detection of a novel mutagen, 3,6-dinitrobenzo[*e*]pyrene, as a major contaminant in surface soil in Osaka and Aichi Prefectures, Japan, Chem. Res. Toxicol. 18 (2005) 283–289.
[33] R. Nakagawa, K. Horikawa, N. Sera, Y. Kodera, H. Tokiwa, Dinitrofluoranthene: induction, identification and gene mutation, Mutat. Res. 191 (1987) 85–91.
[34] K. Takahashi, M. Asanoma, S. Yoshida, G. Ning, H. Mori, T. Horibe, T. Watanabe, T. Hirayama, H. Nukaya, T. Mizutani, Identification of 1,3,6-trinitropyrene as a major mutagen in organic extracts of surface soil from Nagoya city, Japan, Genes Environ. 28 (2006) 160–166.
[35] T. Yahagi, M. Nagao, Y. Seino, T. Matsushima, T. Sugimura, M. Okada, Mutagenicity of *N*-nitrosamines on *Salmonella*, Mutat. Res. 48 (1977) 121–130.
[36] D.M. Maron, B.N. Ames, Revised methods for the *Salmonella* mutagenicity test, Mutat. Res. 113 (1983) 173–215.

[37] A.P. Li, J.S. Dutcher, Mutagenicity of mono-, di- and trinitropyrenes in Chinese hamster ovary cells, Mutat. Res. 119 (1983) 387–392.

[38] M. Nakayasu, H. Sakamoto, K. Wakabayashi, M. Terada, T. Sugimura, Potent mutagenic activity of nitroarenes on Chinese hamster lung cells with diphtheria toxin resistance as a selective marker, Carcinognesis 3 (1982) 917–922.

[39] A. Matsuoka, K. Horikawa, N. Yamazaki, N. Sera, T. Sofuni, H. Tokiwa, Chromosomal aberrations induced in vitro by 3,7- and 3,9-dionitrofluoranthene, Mutat. Res. 298 (1993) 255–259.

[40] K. Horikawa, N. Sera, T. Otofuji, K. Murakami, H. Tokiwa, M. Iwanaga, K. Izumi, H. Otsuka, Pulmonary carcinogenicity of 3,9- and 3,7-dinitrofluoranthene, 3-nitrofluoranthene and benzo[*a*]pyrene in F344 rats, Carcinognesis 12 (1991) 1003–1007.

[41] IARC, IARC Monographs on the evaluation of carcinogenic risks to humans, vol. 65: Printing processes and printing inks, carbon black and some nitro compounds, International Agency for Research on Cancer, Lyons, France, 1996.

Inhibition of peroxisome proliferator-activated receptor γ activity suppresses pancreatic cancer cell motility

Atsushi Nakajima,[1,6] Ayako Tomimoto,[1] Koji Fujita,[1] Michiko Sugiyama,[1] Hirokazu Takahashi,[1] Ikuko Ikeda,[1] Kunihiro Hosono,[1] Hiroki Endo,[1] Kyoko Yoneda,[1] Hiroshi Iida,[1] Masahiko Inamori,[1] Kensuke Kubota,[1] Satoru Saito,[1] Noriko Nakajima,[2] Koichiro Wada,[3] Yoji Nagashima[4] and Hitoshi Nakagama[5]

[1]Division of Gastroenterology, Yokohama City University School of Medicine, 3-9 Fuku-ura, Kanazawa-ku, Yokohama; [2]Department of Pathology, National Institute of Infectious Diseases, 1-23-1 Toyama, Shinjuku-ku, Tokyo; [3]Department of Pharmacology, Graduate School of Dentistry, Osaka University, 1-8 Yamadaoka, Suita, Osaka; [4]Department of Molecular Pathology, Yokohama City University Graduate School of Medicine, 3-9 Fuku-ura, Kanazawa-ku, Yokohama; [5]Biochemistry Division, National Cancer Center Research Institute, 1-1 Tsukiji 5-chome, Chuo-ku, Tokyo, Japan

(Received March 30, 2008/Revised June 6, 2008/Accepted June 9, 2008/Online publication October 9, 2008)

Peroxisome proliferator-activated receptor γ (PPARγ) is a ligand-activated transcription factor that has been implicated in the carcinogenesis and progression of various solid tumors, including pancreatic carcinomas. We aimed to clarify the role of this receptor in pancreatic cell motility *in vitro* and in metastasis *in vivo*. Cell motility was examined by assaying transwell migration and wound filling in Capan-1 and Panc-1 pancreatic cancer cells, with or without the PPARγ-specific inhibitor T0070907. A severe combined immunodeficiency xenograft metastasis model was used to examine the *in vivo* effect of PPARγ inhibition on pancreatic cancer metastasis. In both transwell-migration and wound-filling assays, inhibition of PPARγ activity suppressed pancreatic cell motility without affecting *in vitro* cell proliferation. Inhibition of PPARγ also suppressed liver metastasis *in vivo* in metastatic mice. In PPARγ-inhibited cells, p120 catenin accumulation was induced predominantly in cell membranes, and the Ras-homologous GTPases Rac1 and Cdc42 were inactive. Inhibition of PPARγ in pancreatic cancer cells decreased cell motility by altering p120ctn localization and by suppressing the activity of the Ras-homologous GTPases Rac1 and Cdc42. Based on these findings, PPARγ could function as a novel target for the therapeutic control of cancer cell invasion or metastasis. (*Cancer Sci* 2008; 99: 1892–1900)

Pancreatic ductal adenocarcinoma is associated with one of the highest mortality rates in patients with malignancies.[1] Because of a lack of early symptoms, PDAC is often diagnosed only after a local tumor has disseminated and metastatic disease has already developed in regional lymph nodes or distant organ sites. To overcome this dismal situation, development of novel PDAC therapies involving drugs that target disease-specific molecules is urgently required. PPARγ, a member of the nuclear receptor family of ligand-activated transcription factors, is one promising target for such therapies.[2]

Activation of PPARγ, which is expressed mainly in adipose tissue, is known to play a central role in adipocyte differentiation and insulin sensitivity.[3] For this reason, synthetic PPARγ-activating ligands such as TZD are used commonly as oral antihyperglycemic agents to control non-insulin-dependent diabetes mellitus. More recently, PPARγ has been investigated as a target for the treatment of a variety of cancers.[4–6] The fact that PPARγ is overexpressed in many tumors, including examples in the esophagus, stomach, breast, lung, and colon, suggests that PPARγ function impacts tumor survival.[4–8] Initial efforts to alter PPARγ activity focused on activation with TZD ligands, which have been shown to induce G_1 cell-cycle arrest in a variety of tumor cell lines.[9,10] However, the reported benefits of TZD for pancreatic carcinoma patients in clinical trials are modest at best.[11,12]

Several observations suggest that inhibition of PPARγ function may be beneficial in treating neoplasms.[13,14] Although PPARγ is overexpressed in many cancer cell types, loss-of-function mutations are rare,[15] which suggests that the receptor is a tumor cell survival factor. Evidence that PPARγ function can contribute to carcinogenesis or cancer cell survival includes reports of a murine colon cancer model in which PPARγ activation leads to increased tumor formation.[16,17]

Profiles of PPARγ expression in a variety of human malignancies, including pancreatic cancer, have been described. One recent report showed a significant association between high levels of PPARγ expression in pancreatic cancer cells and shorter overall survival time.[18] Prior investigations demonstrating that PPARγ inhibition induces apoptosis in epithelial tumor lines suggest strongly that PPARγ inhibition may also be beneficial in PDAC treatment.[19–21] In hepatocellular carcinoma cell lines, PPARγ inhibitors have been shown to inhibit cell adhesion and induce morphological changes that normally occur prior to the commitment to apoptosis; in contrast, caspase inhibitors do not prevent these changes.[20] We hypothesize that PPARγ inhibition interferes with adhesion-dependent epithelial cell survival signals, leading to cell death (anoikis). Two additional reports have shown that high doses of PPARγ inhibitors also interfere with Caco-2 cell survival.[22,23] The effect of PPARγ inhibitors (especially at low concentrations) on pancreatic cancer cells has not been investigated.

Ras-homologous GTPases play a pivotal role in the regulation of numerous cellular functions associated with malignant transformation and metastasis. Members of the Rho family of small GTPases are key regulators of actin reorganization and cell motility, as well as cell–cell and cell–extracellular matrix adhesion. These processes all play critical roles during the development and progression of cancer. Because of their pleiotropic functions, Rho proteins appear to be promising targets for the development of novel anticancer drugs,[24,25] including those for PDAC.[25] The ability to modulate pathways regulated by Rho could not only improve the therapeutic efficiency, but also reduce the side effects of conventional antineoplastic therapies.

[6]To whom correspondence should be addressed. E-mail: nakajima-tky@umin.ac.jp
Abbreviations: FITC, fluoresceinisothiocyanate; GST, glutathione-S-transferase; MTT, 3-[4,5-dimethylthiazol-2-yl]-2,5-diphenyltetrazolium bromide; p120ctn, p120 catenin; PDAC, pancreatic ductal adenocaricinoma cells; PPARγ, peroxisome proliferator-activated receptor γ; PPRE, PPARγ-response element; Rho, Ras-homologous; SCID, severe combined immunodeficiency; siRNA, small interfering RNA; TZD, thiazolizinedione.

doi: 10.1111/j.1349-7006.2008.00904.x

The protein p120ctn is the prototypic member of a subfamily of armadillo repeat-domain proteins involved in intercellular adhesion. A recent report demonstrated clearly that p120 regulates, at least in part, the activity of Rho GTPases, and that p120 association with classical cadherins regulates their stability.[26] Ectopic expression of p120ctn has been shown to promote cell migration and to induce a wide variety of morphological changes.[26]

In the present study, we investigated the effects of PPARγ inhibitors on pancreatic cell lines and xenograft metastatic tissues that function as models for PDAC. Our data demonstrate that inhibition of PPARγ in pancreatic cancer cells decreases cell motility by altering p120ctn localization and suppressing the activity of the Rho GTPases Rac1 and Cdc42. These findings suggest that PPARγ inhibitors may improve the benefit of current PDAC therapeutics.

Materials and Methods

Cell lines and reagents. The PDAC cell line Panc-1 was purchased from the American Type Culture Collection (Rockville, MD, USA). Other cell lines were provided by the Cell Resource Center for Biomedical Research, Tohoku University (Sendai, Japan). All cell lines were grown in RPMI-1640 (Sigma-Aldrich, St Louis, MO, USA) supplemented with 10% fetal bovine serum. Cells were maintained at 37°C in an atmosphere of humidified air with 5% CO_2. The PPARγ-specific inhibitor T0070907 and PPARγ ligand rosiglitazone were purchased from Cayman Chemical (Ann Arbor, MI, USA).

Western blot analysis. Adherent cells were washed in phosphate-buffered saline, and cell extracts were prepared in Laemmli lysis buffer. Protein concentrations were measured using Bio-Rad Protein Assay Reagent (Bio-Rad, Richmond, CA, USA) following the manufacturer's suggested procedure. After electrophoresis of extract aliquots (20 μg protein) on 10% sodium dodecylsulfate–polyacrylamide gels, proteins were transferred to nitrocellulose membranes (Millipore, Bedford, MA, USA), blocked at room temperature for 1 h in Tris-buffered saline with 5% bovine serum albumin, and then incubated with primary monoclonal antibody for 1 h. Anti-PPARγ antibody (E-8) was purchased from Santa Cruz Biotechnology (Santa Cruz, CA, USA); monoclonal antibodies against p120ctn and Rac1 were obtained from BD Transduction Laboratories (Palo Alto, CA, USA). After three washes the membranes were incubated for 1 h at room temperature with secondary antibody, and immune complexes were visualized using the enhanced chemiluminescence detection kit (Amersham, London, UK) following the manufacturer's procedure. Images were captured and analyzed using a LAS-3000 imaging system (Fujifilm, Tokyo, Japan). The ProteoExtract Subcellular Proteome Extraction Kit (EMD Biosciences, Darmstadt, Germany) was used for the preparation of cytosolic protein extracts.

Cell proliferation and apoptosis assays. Cell proliferation was measured using MTT assays.[27] Approximately 5×10^3 cells in 100 μL medium were plated per well in a 96-well plate. After 24 h incubation, the medium was changed and supplemented with various concentrations of T0070907 in dimethylsulfoxide, and the cells were incubated for another 24–72 h. After incubating the plates for an additional 4 h with MTT solution (0.5%), sodium dodecylsulfate was added to a final concentration of 20% and absorbance at 595 nm was determined for each well using a microplate reader (Model 550; Bio-Rad). Control wells were treated with dimethylsulfoxide alone. Three independent experiments were carried out for each cell line. Annexin V staining with the annexin V–FITC apoptosis detection kit (Becton Dickinson, San Jose, CA, USA) followed by FACScan flow cytometry (Becton Dickinson) was used to identify apoptotic cells. Apoptosis measures were carried out in triplicate.

Cell-motility assays. Motility was assessed by migration of cells in porous-membrane culture inserts (8.0-μm pore size; Becton Dickinson). After 24 h of incubation, cells that did not migrate were removed from the upper surface of the membrane with a cotton swab, and migrating cells on the lower surface of the membrane were fixed and stained with toluidine blue. Migrating cell counts were estimated from counts of three independent microscopic visual fields (×100). To estimate cell-migration activity during wound healing, cells were grown for 2 days (to confluency), after which a scrape in the form of a cross was made through the confluent monolayers with a plastic pipette tip. To measure migration, several wounded areas within each plate were marked for orientation and then photographed periodically by phase-contact microscopy for 24 h after wounding.

Inhibition of PPARγ function using siRNA. PPARγ siRNA was purchased from Santa Cruz Biotechnology. Panc-1 and Capan-1 cells at 70% confluence were transfected with PPARγ siRNA using Lipofectamine 2000 (Invitrogen, Carlsbad, CA, USA) in accordance with the manufacturer's protocol. The cells were treated with 10 nmol/L PPARγ siRNA for 24 h. Stealth RNAi Negative Control Medium GC (Invitrogen) was used for control specimens. Using real-time reverse transcription–polymerase chain reaction to measure steady-state mRNA levels in cells, PPARγ-specific siRNA was found to inhibit PPARγ expression to levels less than 30% of those in control cells (data not shown).

Measuring the effect of T0070907 on PPARγ-dependent transcription. Capan-1 cells transfected with plasmid encoding a PPARγ-response element fused to a luciferase reporter (pHD[×3]PPRE-Luc) were stimulated as described previously with 1 μmol/L rosiglitazone and various concentrations of T0070907.[20] Luciferase activity was measured 16 h after transfection. Because Renilla luciferase control plasmids are sensitive to steroid/thyroid/retinoid nuclear–receptor stimulation, variability in transfection efficiencies (<20%) were assessed in parallel experiments using the pRL-TK plasmid (Promega, Madison, WI, USA).

Immunofluorescence staining. Cells (5×10^5 per well) were grown on collagen-1-coated glass coverslips in six-well flat-bottom plates for 24 h. After 24 h incubation, T0070907 was added to a final concentration of 0.1 μmol/L and the cells were grown for an additional 24 h. The cells were then fixed in 4% paraformaldehyde followed by 100% ethanol at –20°C. After permeabilization with 0.1% Triton-X, non-specific binding of antibody to the cells was blocked with 2% normal swine serum. Cells were incubated subsequently with anti-p120 catenin antibody followed by FITC-labeled secondary antibody. Samples were then mounted using Vectashield (Vector Laboratories, Burlingame, CA, USA) and examined using confocal laser-scanning microscopy (Carl Zeiss, Oberkochen, Germany). All experiments were repeated in triplicate.

Measurement of Rac-1 and Cdc42 activities. GST pull-down assays using a Rac-1/Cdc42 activation kit were used to evaluate Rac1/Cdc42 activities according to the manufacturer's protocol (Stressgen, Ann Arbor, MI, USA). Briefly, we used a GST fusion polypeptide composed of GST fused to the interactive domain of human p21-activated kinase-1, which interacts specifically with GTP-bound Cdc42 and Rac1 GTPases.[25] The GST fusion target was incubated with cell lysates and then applied to GST-specific beads to estimate the relative abundance of active Cdc42 and Rac1. Bound Rac1 and Cdc42 proteins were resolved on 12% denaturing polyacrylamide gels and distinguished by western blotting using antibodies specific to each protein. The amount of active GTP-bound enzyme was quantified relative to the total amount of each GTPase present in whole unprecipitated cell lysates. The experiments were carried out six times.

***In vivo* metastasis study.** Five-week-old male SCID mice were obtained from CLEA Japan (Tokyo, Japan) and maintained in a

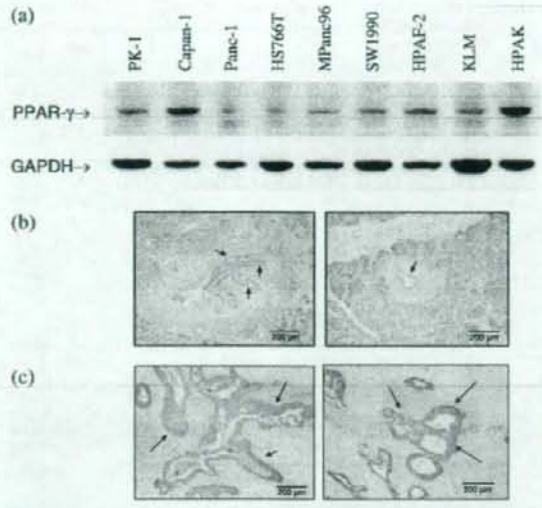

Fig. 1. Expression of peroxisome proliferator-activated receptor γ (PPARγ) in pancreatic cancer cells. (a) Western blots showing PPARγ expression in various pancreatic ductal adenocarcinoma cell lines, as well as a glyceraldehyde-3-phosphate dehydrogenase (GAPDH) internal control. Immunohistochemical staining of (b) normal ductal epithelium (left and right panels) and (c) pancreatic ductal adenocarcinoma (left and right panels) with anti-PPARγ antibody. Arrows mark staining of normal pancreatic ductal epithelium in (b) and pancreatic ductal adenocarcinoma in (c).

specific pathogen-free environment. Experiments were carried out according to the guidelines of Yokohama City University. Six-week-old mice were used in this experiment. To assay metastatic capability, viable cancer cells were suspended in serum-free medium, and 20-μL aliquots of cell suspension containing 2×10^6 cells were inoculated into the spleens of SCID mice under anesthesia. After inoculation, the mice were randomized into two treatment groups ($n = 6$) and one control group ($n = 6$). Administration of T0070907 (5 mg/kg/day) to each treatment group began 1 day after cell inoculation and continued daily for 4 weeks. Four weeks after inoculation, the mice were killed and autopsied immediately. Liver metastasis was measured by counting macroscopic lesions, and measuring them to calculate tumor volume:

$$\text{length}/2 \times \text{width}/2 \times \text{height}/2 \times 4/3 \times \pi.^{(28)}$$

Examination of hematoxylin–eosin-stained sections of each lesion resulted in assessments of histopathological alterations in liver metastases.

Results

Expression of PPARγ in pancreatic ductal adenocarcinoma cells. Western blotting of PPARγ with the E8 antibody revealed a specific band between 50 and 60 kDa present in all PDAC cell lines examined (Fig. 1a). Among these lines, steady-state levels of PPARγ protein were highest in Capan-1 and HPAK cells, and lowest in Panc-1 and HS766T cells. Immunohistochemical staining with a PPARγ-specific antibody demonstrated that PPARγ expression in PDAC tissues (Fig. 1c) was similar to normal pancreatic ductal epithelium (Fig. 1b).

Peroxisome proliferator-activated receptor γ inhibitors reduce migration of PDAC cells. The effect of the PPARγ antagonist T0070907 on PDAC cell migration was measured using *in vitro* wound-filling assays. The migration of wounded cells treated with T0070907 was inhibited significantly (Fig. 2a,b) relative to untreated, wounded Panc-1 and Capan-1 cells. Among cells transfected with PPARγ siRNA to reduce PPARγ expression levels, Capan-1 cell migration was more severely inhibited than Panc-1 (Fig. 2c,d). These results indicate that chemical inhibitors or inhibitory siRNA molecules that reduce PPARγ activity lead to inhibition of wound filling. Migration of Capan-1 and Panc-1 cells in the absence or presence of several concentrations of T0070907 were also measured in 24-h transwell migration assays (Fig. 3). In both cell lines, the presence of T0070907 reduced cell migration significantly and in a dose-dependent manner (Fig. 3a,c). Reduced migration of cells with PPARγ siRNA relative to untreated controls (Fig. 3b,d) demonstrates that transwell migration is inhibited specifically by a reduction in PPARγ activity.

Effect of PPARγ inhibitor on cell proliferation and apoptosis. To investigate whether chemical inhibition of PPARγ affects cancer cell proliferation and apoptosis, we used MTT assays to measure cell proliferation and apoptosis in cultured Panc-1 and Capan-1 PDAC cell lines. No significant changes in cell proliferation (Fig. 4a,b) or apoptosis (Fig. 4c,d) were observed in T0070907-treated versus untreated PDAC cells. These results demonstrate that suppression of cell proliferation or apoptosis is not necessarily consequent to T0070907-mediated suppression of PDAC cell motility.

Inhibition of PPARγ alters the subcellular localization of p120ctn. Association of p120ctn with the intracellular domains of cadherins promotes cell–cell adhesion and cell motility by regulating the activation of Rho GTPases.[29,30] Because cytoplasmic p120ctn is the only known activator of Rho GTPases that functions in cell motility, the ratio of cadherin-bound p120ctn to p120ctn in the cytplasmic pool is an important factor regulating motility. To examine the involvement of p120ctn in T0070907-mediated suppression of cell motility, we used immunocytochemical analyses to examine the subcellular distribution of p120ctn in PDAC cells. In T0070907-treated Capan-1 cells, p120ctn was found predominantly on the plasma membranes (relative to more free p120ctn in the cytoplasm of untreated cells) (Fig. 5a). In contrast, there were no significant changes in the distribution of p120ctn in T0070907-treated Panc-1 cells (data not shown). The intracellular distributions of PPARγ and p120ctn did not overlap (merged) (Fig. 5a).

Although western blots of fractionated cells revealed that cytoplasmic p120ctn levels decreased in T0070907-treated Capan-1 cells (Fig. 5b), no significant change in distribution was observed between untreated and treated Panc-1 cells (data not shown). These results indicate that in Capan-1 cells, PPARγ inhibition increases the relative amount of cadherin-bound p120ctn. We speculate that relatively low levels of PPARγ expression in Panc-1 cells may confound our ability to measure any similar change in p120ctn subcellular localization following T0070907 treatment. To investigate whether PPARγ activity in Capan-1 cells is inhibited by low concentrations of T0070907, the effect of a range of T0070907 concentrations on PPRE-dependent transcription was measured (Fig. 5c). With 0.1 μmol/L T0070907, PPRE-dependent transcription in Capan-1 cells was inhibited to approximately half maximum.

Peroxisome proliferator-activated receptor γ inhibitor suppresses the activity of Rac-1 and Cdc42. Previous reports suggest that p120ctn affects cell motility in association with Rac1 and Cdc42 Rho GTPases.[30-33] The activities of Rac1 and Cdc42 GTPases were measured in lysates of T0070907-treated and -untreated Capan-1 cells using a GST pull-down target that interacts specifically with active GTPases. In T0070907-treated cells, we observed a significant decrease in the percent-active fractions of Rac1 and Cdc42 GTPases (Fig. 6).

doi: 10.1111/j.1349-7006.2008.00904.x

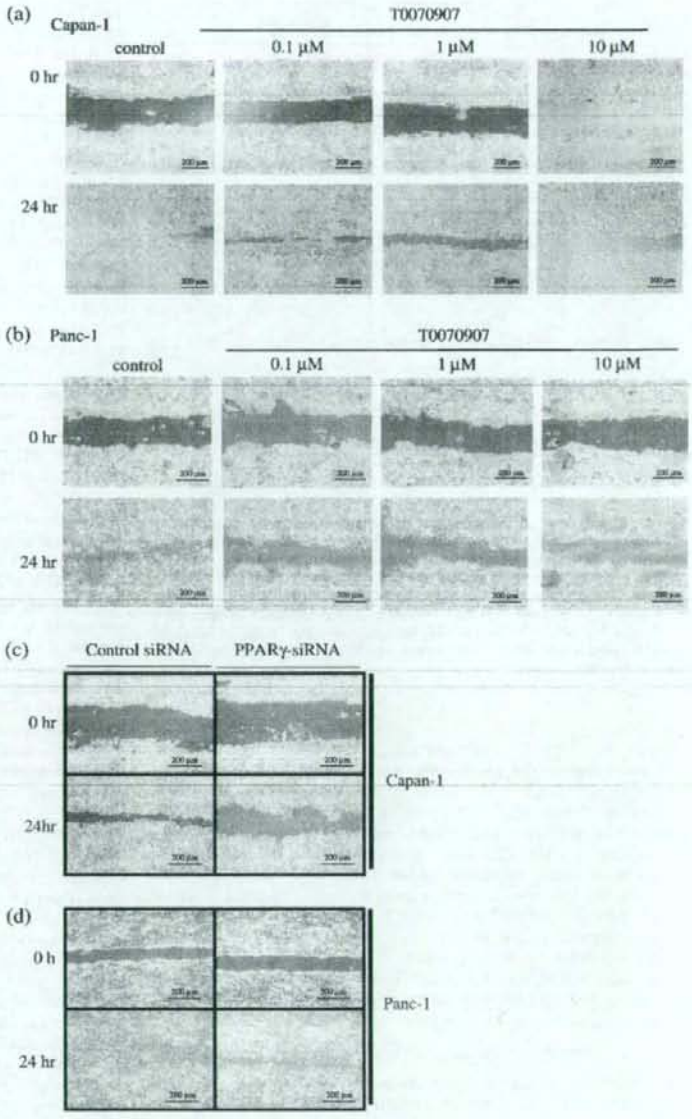

Fig. 2. Peroxisome proliferator-activated receptor γ (PPARγ) inhibition reduces the wound-filling ability of PDAC cells. Wound-filling assays in (a) Capan-1 and (b) Panc-1 cells treated with various concentrations of T0070907 for 24 h. In both lines, all concentrations of PPARγ inhibitor result in slower cell migration into wound areas. (c) Capan-1 and (d) Panc-1 cells transfected with PPARγ small interfering RNA (siRNA) also migrated more slowly into wound areas than cells transfected with control siRNA.

Peroxisome proliferator-activated receptor γ inhibitor reduces liver metastasis in a mouse xenograft model. To investigate whether PPARγ inhibitors affect metastatic cell spreading, we tested the ability of T0070907 to reduce metastatic tumor formation in a Capan-1/SCID mouse xenograft model. Capan-1 cells were injected into the spleens of SCID mice, and the number and size of metastatic lesions in livers were measured after 4 weeks (Fig. 7). Mice treated orally with 5 mg/kg/day of T0070907 contained two-thirds fewer metastatic foci ($P < 0.05$), with an average tumor volume of only 12% of tumors in control mice ($P < 0.05$) (Table 1). Serum L-alanine aminotransferase (ALT) levels were within the normal range in the all mice (Suppl. Fig. S1).

Discussion

We demonstrated that levels of PPARγ expression vary among pancreatic adenocarinoma cell lines (Fig. 1) and tested the effect of the PPARγ-specific inhibitor T0070907 on PDAC cells. In Capan-1 and Panc-1 cells, both T0070907 and PPARγ siRNA suppressed cell motility, migration, and invasion, but did not inhibit cell proliferation (Figs 2–4). These results suggest strongly that PPARγ plays a crucial role in PDAC cell motility, migration, and invasion. Elucidating the mechanism that underlies cell motility is of clinical importance as a means for controlling tumor cell invasion, dissemination, and metastasis in patients with pancreatic cancer.

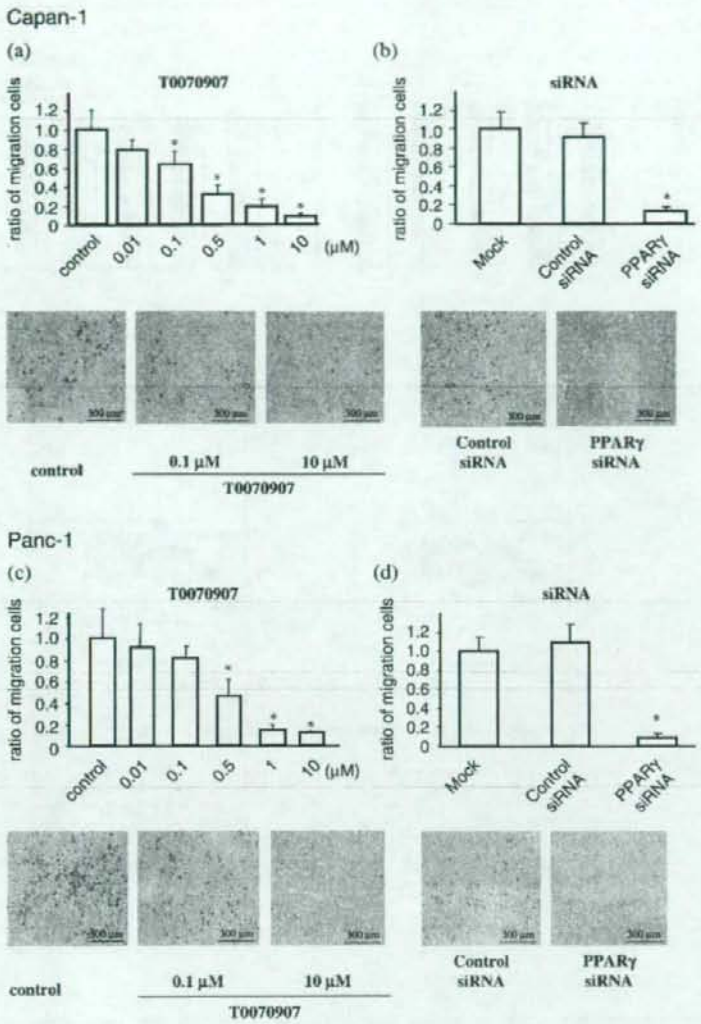

Fig. 3. Peroxisome proliferator-activated receptor γ (PPARγ) inhibition reduces migration of PDAC cells. Cell migrations were estimated from transwell migration assays, in which migrated cells are stained violet and membrane pores can be seen as white dots. Relative to control-treated cells, (a) Capan-1 and (c) Panc-1 cell migration decreased significantly and in a dose-dependent manner in response to increasing concentrations of PPARγ inhibitor T0070907 (*$P < 0.05$). (b,d) Significant decreases in cell migration were also observed in PPARγ small interfering RNA (siRNA)-transfected cells relative to control siRNA-transfected cells.

Table 1. Effects of peroxisome proliferator-activated receptor γ inhibitor (T0070907) on liver metastasis of Capan-1 cells

Incidence	Number of metastatic colonies (mean ± SD)	Total tumor volume (mm^3) (mean ± SD)
Vehicle	3.50 ± 1.05	738.6 ± 415.7
T0070907 (5 mg/kg/day)	1.00 ± 1.27	86.8 ± 173.2
	$P < 0.05$	$P < 0.05$

Capan-1 cells were injected into the spleen of male severe combined immunodeficiency mice. One day after injection, three groups ($n = 6$) were randomized into vehicle or 5 mg/kg/day T0070907. After 4 weeks, livers were harvested, and the number of metastases and total tumor volume of all metastatic lesions was determined.

Following treatment with T0070907 PPARγ inhibitor, p120ctn was found predominantly in Capan-1 cell membranes. Recent reports demonstrate that p120ctn associates with all classic cadherin subtypes, and is involved in the regulation of cell motility and cell adhesion.[26] p120ctn is known to also regulate actin cytoskeleton configuration. We did not observe colocalization of PPARγ and p120ctn expression in PPARγ inhibitor-treated or -untreated cells, indicating that PPARγ may not interact directly with p120ctn.

doi: 10.1111/j.1349-7006.2008.00904.x

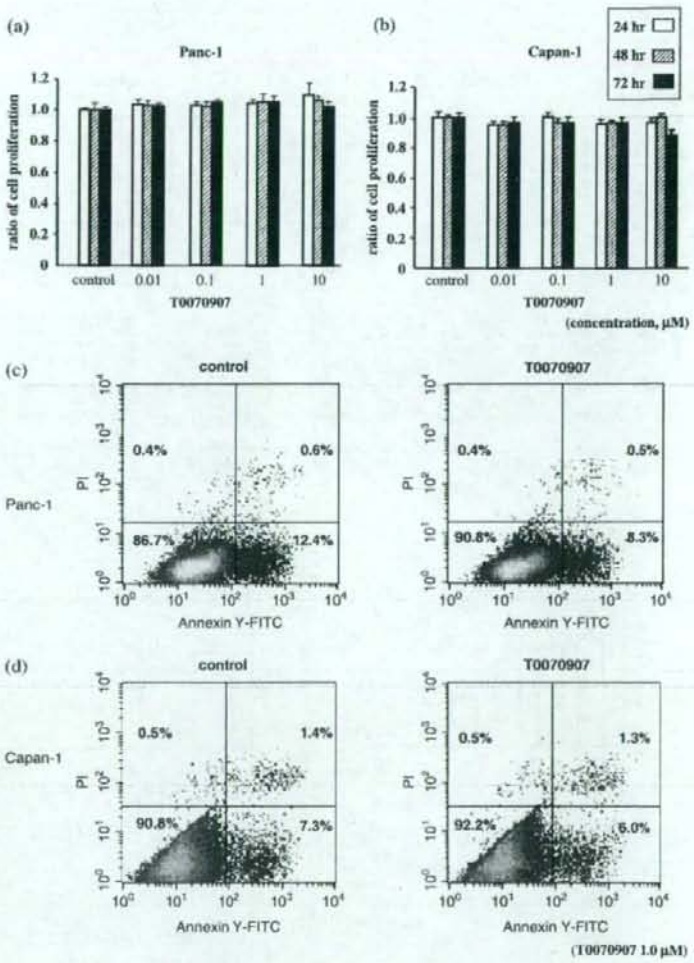

Fig. 4. Effect of a peroxisome proliferator-activated receptor γ (PPARγ) inhibitor on cell proliferation and apoptosis in PDAC cells. Cell proliferation was calculated from 3-[4,5-dimethylthiazol-2-yl]-2,5-diphenyltetrazolium bromide (MTT) assays. (a) Panc-1 and (b) Capan-1 cells treated with 1.0 μmol/L T0070907 for 24, 48, and 72 h showed no significant change in MTT values relative to control cells (*y*-axis values represent the ratio of MTT optical density readings from treated and untreated cells; columns represent ratio mean ± SD). Apoptotic cell counts were measured by fluorescence activated cell sorting (FACS) after treatment of (c) Panc-1 or (d) Capan-1 cells without or with 1.0 μmol/L T0070907 for 24 h. T0070907 treatments did not result in any significant changes in the percentage of apoptotic cells.

Ras-homologous GTPases, which localize to membranes in a GDP-bound state, are activated to a GTP-bound state upon stimulation of cell-surface receptors. Upon activation, Rho GTPases bind effectors that trigger specific cellular responses. As Rho proteins are known to play essential roles in signaling events that regulate cadherin-dependent motility, specific inhibitors of individual Rho functions (notably RhoA-, RhoB-, Rac1-, or Cdc42-related functions) could provide therapeutic benefits in controlling cancer metastasis. Indeed, compounds developed as specific inhibitors of the RhoA-effector molecule Rho-kinase have been demonstrated to exert antimetastatic activity *in vivo*.[24]

The inactivation of Rac1 and Cdc42 that we observed in response to PPARγ inhibition indicates that these molecules are involved in PPARγ-mediated PDAC cell motility. We also demonstrated liver metastasis inhibition in response to PPARγ inhibition in an *in vivo* metastatic model. Previous reports have demonstrated an induction in apoptosis in response to PPARγ inhibition in other epithelial tumor lines.[19–21] Anoikis, which is a loss of adhesion-induced apoptosis, was also reported in response to PPARγ inhibition by T0070907; however, concentrations greater than 10 μmol/L T0070907 have been shown to be required to induce anoikis in a variety of carcinoma cell lines. In the present study, we observed a significant inhibitory effect of T0070907 on cell migration at much lower T0070907 concentrations (0.01–1 μmol/L; Fig. 5c) that had no effect on cell proliferation or cell death as measured in MTT and apoptosis assays (Fig. 4). Our findings at low concentrations of T0070907 suggest that inhibition of cancer cell migration is due to the specificity of T0070907's pharmacological effect on PPARγ, and not by anoikis, which is induced at higher concentrations of PPARγ inhibitor. The relatively low concentrations of T0070907 required for inhibition and the dose-dependent effect of the inhibitor on cell migration make it unlikely that inhibition was non-specific.

Transwell migration and wound-filling assays in both Capan-1 and Panc-1 pancreatic cancer cell lines demonstrated the inhibitory effects of PPARγ on cell motility *in vitro*. In contrast, the effects of PPARγ inhibitor on p120ctn subcellular localization, and on Rac1 and Cdc42 GTPase activities, were exclusive to Capan-1 cells, and not seen in Panc-1. We speculate that relative

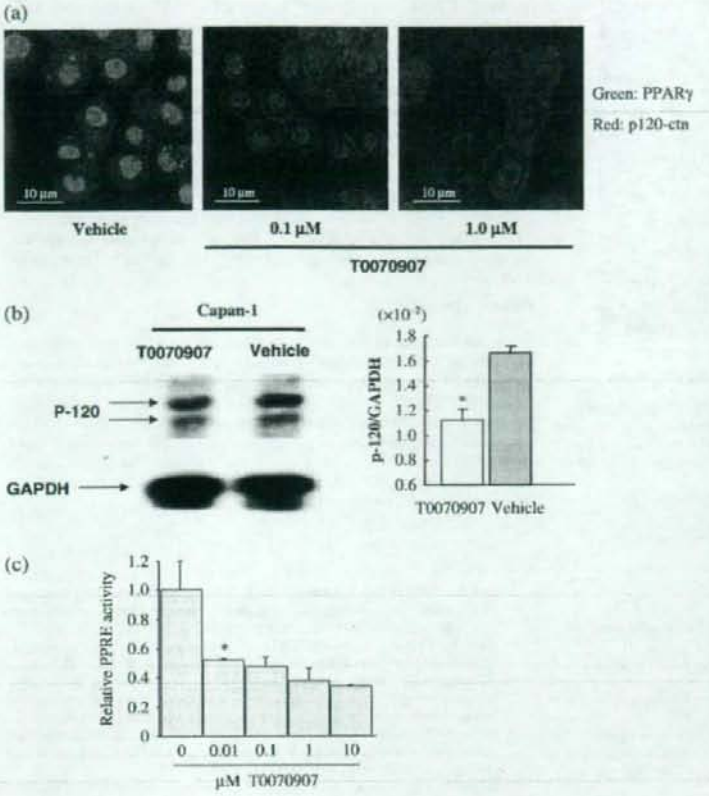

Fig. 5. Peroxisome proliferator-activated receptor γ (PPARγ) inhibitor T0070907 affects the subcellular localization of p120 catenin (p120ctn) in Capan-1 cells. (a) The subcellular distribution of p120ctn in Capan-1 control cells or those treated with 0.1 or 1.0 μmol/L T0070907 were compared following immunostaining with antip120ctn (red) and anti-PPARγ (green). Although p120ctn accumulated in the cytoplasm of vehicle-treated cells, it localized predominantly to cell membranes in T0070907-treated Capan-1 cells. Merged images of PPARγ and p120ctn immunohistochemical staining patterns show no colocalization. (b) Western-blot analysis of cytosolic protein extracts with p120ctn antibody and glyceraldehyde-3-phosphate dehydrogenase (GAPDH) control antibody. T0070907 treatment resulted in reduced signal strength from the cytosolic p120ctn band. Changes in the cytosolic p120ctn expression can be seen by the reduction in the ratio of p120ctn : GAPDH signal. Bars represents the mean ratio of p120 : GAPDH signal strength ± SD. $^*P < 0.05$. (c) Capan-1 cells transfected with a PPARγ-response element (PPRE)-luciferase reporter plasmid were stimulated with 1 mmol/L rosiglitazone (synthetic ligand of PPARγ) in the presence of concentrations of T0070907 shown. Luciferase activity was measured after 16 h of treatment. Bars represent relative PPRE activity as measured by the ratio of PPARγ-dependent luciferase activity in treated cells relative to untreated cells.

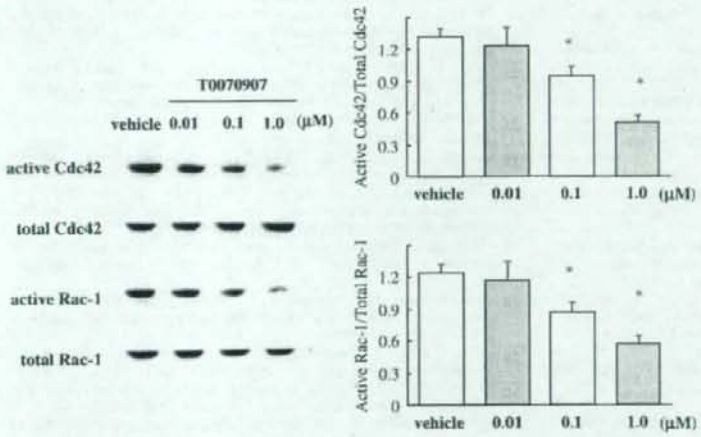

Fig. 6. Effect of the peroxisome proliferator-activated receptor γ (PPARγ) inhibitor T0070907 on the activity of Rac-1 and Cdc42 GTPases in Capan-1 cells. GTPase activity for Rac-1 and Cdc42 was measured using GST pull-down assays that are capable of distinguishing the percentage of the active fraction (relative to total) of Rac-1 and Cdc42 in lysates of Capan-1 cells. Treatment with T0070907 (0.1 and 1.0 μmol/L) resulted in a significant decrease in the percentage of active Rac-1 and Cdc42. Each column represents the mean ± SD. The experiments were carried out six times. $^*P < 0.05$.

doi: 10.1111/j.1349-7006.2008.00904.x

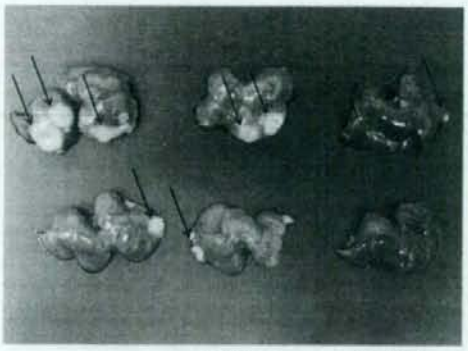

Vehicle | T0070907 (1 mg/kg/day) | T0070907 (5 mg/kg/day)

Fig. 7. Peroxisome proliferator-activated receptor γ (PPARγ) inhibitor T0070907 reduces the number and volume of metastases in a murine xenograft model. Numbers and areas of metastases (arrows) in the liver decreased markedly in mice treated with T0070907 relative to control mice.

to Panc-1 cells, steady-state levels of PPARγ in Capan-1 cells are much higher (Fig. 1a), which may contribute to these discrepancies. This hypothesis is supported by a recent clinical report in which a significant positive association was measured between high levels of PPARγ expression in pancreatic cancer cells and shorter overall survival time.[18] Further investigation will be required to better understand the mechanism of PPARγ inhibition of pancreatic cancer cell motility, invasion, and metastasis.

In conclusion, we have demonstrated that inhibition of PPARγ in pancreatic cancer cells decreases cell motility by altering p120ctn localization and suppressing Rac1 and Cdc42 Rho GTPase activities. PPARγ could function as a novel therapeutic target for controlling cancer cell dissemination or metastasis.

Acknowledgments

We thank Machiko Hiraga and Yuko Satoh for their technical assistance. The present work was supported in part by a Grant-in-Aid for research on the Third Term Comprehensive Control Research for Cancer from the Ministry of Health, Labour and Welfare, Japan to A.N., a grant from the National Institute of Biomedical Innovation to A.N., a grant from the Ministry of Education, Culture, Sports, Science and Technology, Japan (KIBAN-B) to A.N., a grant from the Princess Takamatsu Cancer Research Foundation to A.N., and a grant from the Japanese Human Science Research Foundation to A.N.

References

1 Jemal A, Siegel R, Ward E, Murray T, Xu J, Thun MJ. Cancer statistics, 2007. *CA Cancer J Clin* 2007; **57**: 43–66.
2 Kersten S, Desvergne B, Wahli W. Roles of PPARs in health and disease. *Nature* 2000; **405**: 421–4.
3 Desvergne B, Wahli W. Peroxisome proliferator-activated receptors: nuclear control of metabolism. *Endocr Rev* 1999; **20**: 649–88.
4 Takashima T, Fujiwara Y, Higuchi K *et al.* PPAR-γ ligands inhibit growth of human esophageal adenocarcinoma cells through induction of apoptosis, cell cycle arrest and reduction of ornithine decarboxylase activity. *Int J Oncol* 2001; **19**: 465–71.
5 Chang TH, Szabo E. Induction of differentiation and apoptosis by ligands of peroxisome proliferator-activated receptor gamma in non-small cell lung cancer. *Cancer Res* 2000; **60**: 1129–38.
6 DuBois RN, Gupta R, Brockman J, Reddy BS, Krakow SL, Lazar MA. The nuclear eicosanoid receptor, PPARγ, is aberrantly expressed in colonic cancers. *Carcinogenesis* 1998; **19**: 49–53.
7 Mueller E, Sarraf P, Tontonoz P *et al.* Terminal differentiation of human breast cancer through PPAR gamma. *Mol Cell* 1998; **1**: 465–70.
8 Sato H, Ishihara S, Kawashima K *et al.* Expression of peroxisome proliferator-activated receptor (PPAR) γ in gastric cancer and inhibitory effects of PPARγ agonists. *Br J Cancer* 2000; **83**: 1394–400.
9 Guan YF, Zhang YH, Breyer RM, Davis L, Breyer MD. Expression of peroxisome proliferator-activated receptor γ (PPARγ) in human transitional bladder cancer and its role in inducing cell death. *Neoplasia* 1999; **1**: 330–9.
10 Kitamura S, Miyazaki Y, Shinomura Y, Kondo S, Kanayama S, Matsuzawa Y. Peroxisome proliferator-activated receptor γ induces growth arrest and differentiation markers of human colon cancer cells. *Jpn J Cancer Res* 1999; **90**: 75–80.
11 Debrock G, Vanhentenrijk V, Sciot R, Debiec-Rychter M, Oyen R, Van Oosterom A. A phase II trial with rosiglitazone in liposarcoma patients. *Br J Cancer* 2003; **89**: 1409–12.
12 Kulke MH, Demetri GD, Sharpless NE *et al.* A phase II study of troglitazone, an activator of the PPARγ receptor, in patients with chemotherapy-resistant metastatic colorectal cancer. *Cancer J* 2002; **8**: 395–9.
13 Martelli ML, Iuliano R, Le Pera I *et al.* Inhibitory effects of peroxisome poliferator-activated receptor γ on thyroid carcinoma cell growth. *J Clin Endocrinol Metab* 2002; **87**: 4728–35.
14 Panigrahy D, Shen LQ, Kieran MW, Kaipainen A. Therapeutic potential of thiazolidinediones as anticancer agents. *Expert Opin Invest Drugs* 2003; **12**: 1925–37.
15 Posch MG, Zang C, Mueller W, Lass U, von Deimling A, Elstner E. Somatic mutations in peroxisome proliferator-activated receptor-γ are rare events in human cancer cells. *Med Sci Monit* 2004; **10**: BR250–4.
16 Lefebvre AM, Chen I, Desreumaux P *et al.* Activation of the peroxisome proliferator-activated receptor γ promotes the development of colon tumors in C57BL/6J-APCMin/+ mice. *Nat Med* 1998; **4**: 1053–7.
17 Saez E, Tontonoz P, Nelson MC *et al.* Activators of the nuclear receptor PPARγ enhance colon polyp formation. *Nat Med* 1998; **4**: 1058–61.
18 Kristiansen G, Jacob J, Buckendahl AC *et al.* Peroxisome proliferator-activated receptor γ is highly expressed in pancreatic cancer and is associated with shorter overall survival times. *Clin Cancer Res* 2006; **12**: 6444–51.
19 Masuda T, Wada K, Nakajima A *et al.* Critical role of peroxisome proliferator-activated receptor γ on anoikis and invasion of squamous cell carcinoma. *Clin Cancer Res* 2005; **11**: 4012–21.
20 Schaefer KL, Wada K, Takahashi H *et al.* Peroxisome proliferator-activated receptor γ inhibition prevents adhesion to the extracellular matrix and induces anoikis in hepatocellular carcinoma cells. *Cancer Res* 2005; **65**: 2251–9.
21 Takahashi H, Fujita K, Fujisawa T *et al.* Inhibition of peroxisome proliferator-activated receptor γ activity in esophageal carcinoma cells results in a drastic decrease of invasive properties. *Cancer Sci* 2006; **97**: 854–60.
22 Lea MA, Sura M, Desbordes C. Inhibition of cell proliferation by potential peroxisome proliferator-activated receptor (PPAR) γ agonists and antagonists. *Anticancer Res* 2004; **24**: 2765–71.
23 Ramilo G, Valverde I, Lago J, Vieites JM, Cabado AG. Cytotoxic effects of BADGE (bisphenol A diglycidyl ether) and BFDGE (bisphenol F diglycidyl ether) on Caco-2 cells *in vitro*. *Arch Toxicol* 2006; **80**: 748–59.
24 Fritz G, Kaina B. Rho GTPases: promising cellular targets for novel anticancer drugs. *Curr Cancer Drug Targets* 2006; **6**: 1–14.
25 Taniuchi K, Nakagawa H, Hosokawa M *et al.* Overexpressed P-cadherin/CDH3 promotes motility of pancreatic cancer cells by interacting with p120ctn and activating Rho-family GTPases. *Cancer Res* 2005; **65**: 3092–9.
26 Anastasiadis PZ. p120-ctn: a nexus for contextual signaling via Rho GTPases. *Biochim Biophys Acta* 2007; **1773**: 34–46.
27 Mosmann T. Rapid colorimetric assay for cellular growth and survival: application to proliferation and cytotoxicity assays. *J Immunol Meth* 1983; **65**: 55–63.
28 Yasui N, Sakamoto M, Ochiai A *et al.* Tumor growth and metastasis of human colorectal cancer cell lines in SCID mice resemble clinical metastatic behaviors. *Invasion Metastasis* 1997; **17**: 259–69.
29 Nobes CD, Hall A. Rho GTPase control polarity, protrusion, and adhesion during cell movement. *J Cell Biol* 1999; **144**: 1235–44.
30 Noren NK, Liu Bp Burridge K, Kreft B. p120 catenin regulates the actin cytoskeleton via Rho family GTPase. *J Cell Biol* 2000; **150**: 567–80.
31 Nobes CD, Hall A. Rho GTPases control polarity, protrusion, and adhesion during cell movement. *J Cell Biol* 1999; **144**: 1235–44.
32 Noren NK, Liu BP, Burridge K, Kreft B. p120 catenin regulates the actin cytoskeleton via Rho family GTPases. *J Cell Biol* 2000; **150**: 567–80.
33 Anastasiadis PZ, Reynolds AB. Regulation of Rho GTPases by p120-catenin. *Curr Opin Cell Biol* 2001; **13**: 604–10.

Supporting Information

Additional Supporting Information may be found in the online version of this article:

Fig. S1. Serum levels of alanine aminotransferase (ALT) in the T0070907-treated metastatic model mice. There was no liver injury at this dose of T0070907.

Please note: Blackwell Publishing are not responsible for the content or functionality of any supporting materials supplied by the authors. Any queries (other than missing material) should be directed to the corresponding author for the article.

doi: 10.1111/j.1349-7006.2008.00904.x

Adiponectin suppresses colorectal carcinogenesis under the high-fat diet condition

T Fujisawa, H Endo, A Tomimoto, M Sugiyama, H Takahashi, S Saito, M Inamori, N Nakajima, M Watanabe, N Kubota, T Yamauchi, T Kadowaki, K Wada, H Nakagama and A Nakajima

Gut 2008;57;1531-1538; originally published online 1 Aug 2008; doi:10.1136/gut.2008.159293

Adiponectin suppresses colorectal carcinogenesis under the high-fat diet condition

T Fujisawa,[1] H Endo,[1] A Tomimoto,[1] M Sugiyama,[1] H Takahashi,[1] S Saito,[1] M Inamori,[1] N Nakajima,[2] M Watanabe,[3] N Kubota,[4] T Yamauchi,[4] T Kadowaki,[4] K Wada,[5] H Nakagama,[6] A Nakajima[1]

► Additional figures and tables are published online only at http://gut.bmj.com/content/vol57/issue11

[1] Division of Gastroenterology, Yokohama City University School of Medicine, Yokohama, Japan; [2] Department of Pathology, National Institute of Infectious Diseases, Tokyo, Japan; [3] Laboratory for Medical Engineering, Graduate School of Engineering, Yokohama National University, Yokohama, Japan; [4] Department of Internal Medicine, Graduate school of Medicine, University of Tokyo, Tokyo, Japan; [5] Department of Pharmacology, Graduate School of Dentistry, Osaka University, Osaka, Japan; [6] Biochemistry Division, National Cancer Center Research Institute, Tokyo, Japan

Correspondence to: Dr A Nakajima, 3-9 Fukuura, Kanazawa-ku, Yokohama 236-0004, Japan; Nakajima-tky@umin.ac.jp

Revised 4 July 2008
Accepted 22 July 2008
Published Online First 1 August 2008

ABSTRACT

Background and aims: The effect of adiponectin on colorectal carcinogenesis has been proposed but not fully investigated. We investigated the effect of adiponectin deficiency on the development of colorectal cancer.

Methods: We generated three types of gene-deficient mice (adiponectin-deficient, adiponectin receptor 1-deficient, and adiponectin receptor 2-deficient) and investigated chemical-induced colon polyp formation and cell proliferation in colon epithelium. Western blot analysis was performed to elucidate the mechanism which affected colorectal carcinogenesis by adiponectin deficiency.

Results: The numbers of colon polyps were significantly increased in adiponectin-deficient mice compared with wild-type mice fed a high-fat diet. However, no difference was observed between wild-type and adiponectin-deficient mice fed a basal diet. A significant increase in cell proliferative activity was also observed in the colonic epithelium of the adiponectin-deficient mice when compared with wild-type mice fed a high-fat diet; however, no difference was observed between wild-type and adiponectin-deficient mice fed a basal diet. Similarly, an increase in epithelial cell proliferation was observed in adiponectin receptor 1-deficient mice, but not in adiponectin receptor 2-deficient mice. Western blot analysis revealed activation of mammalian target of rapamycin, p70 S6 kinase, S6 protein and inactivation of AMP-activated protein kinase in the colon epithelium of adiponectin-deficient mice fed with high-fat diet.

Conclusions: Adiponectin suppresses colonic epithelial proliferation via inhibition of the mammalian target of the rapamycin pathway under a high-fat diet, but not under a basal diet. These studies indicate a novel mechanism of suppression of colorectal carcinogenesis induced by a Western-style high-fat diet.

Adipose tissue produces and secretes several bioactive substances[1 2] known as adipocytokines,[3] and obesity is an important risk factor for many human diseases, including colorectal cancer and diabetes mellitus.[4 5] Several case–control studies have shown that high-fat diets may promote the development of colorectal cancer,[6] and the results of animal experiments suggest the existence of a link between fat intake and colorectal cancer[7]. Adiponectin is mainly secreted by adipocytes[8] and is a key hormone responsible for insulin sensitisation.[9 10] While adiponectin protein is abundantly found in the plasma of healthy human subjects,[11] adiponectin mRNA levels in the adipose tissue and plasma are dramatically decreased in patients with obesity and/or type 2 diabetes mellitus.[12 13] Because both obesity and type 2 diabetes have been reported to be associated with an elevated risk of colorectal cancer,[14–16] we hypothesised that the plasma level of adiponectin may be related to the risk of colorectal cancer.

Several contradictory results have been reported from human clinical studies on the relationship between the plasma levels of adiponectin and the risk of colorectal cancer.[17 18] While some clinical studies have been conducted in humans, no studies investigating the relationship between the plasma levels of adiponectin and the risk of colorectal cancer have been reported in animal models. Therefore, the mechanism underlying the promotion of colorectal carcinogenesis by adiponectin deficiency still remains unclear.

It is now well known that the adiponectin receptor exists in two isoforms: adiponectin receptor 1 (AdipoR1), which is abundantly expressed in the skeletal muscle; and adiponectin receptor 2 (AdipoR2), which is predominantly expressed in the liver.[19] These receptors mediate the enhanced activation of AMP-activated protein kinase (AMPK) and the peroxisome proliferator-activated receptor α (PPARα), as well as the increase in fatty-acid oxidation and glucose uptake induced by adiponectin.[20 21]

Recently, involvement of the AMPK/mammalian target of rapamycin (mTOR) pathway in the development of various types of cancer has attracted attention.[22–24] The important role of mTOR in mammalian cells is related to its control of mRNA translation. The targets for mTOR signalling are proteins involved in controlling the translational machinery, including the ribosomal protein S6 kinases and S6 proteins that regulate the initiation and elongation phases of translation.[25 26] With regard to the upstream control, mTOR is regulated by signalling pathways linked to several oncoproteins or tumour suppressors, including AMP-activated protein kinase (AMPK).[25–27] mTOR is located at the intersection of major signalling pathways and is believed to be capable of integrating a large panel of stress signals, including nutrient deprivation, energy depletion, and oxidative or hypoxic stresses. In particular, AMPK activation has been reported to directly inhibit mTOR[28] and suppress cell proliferation.

Using adiponectin-deficient mice (KO) we therefore investigated whether adiponectin deficiency might promote the development of colorectal cancer, and examined the involvement of the AMPK/mTOR pathway in the effect of adiponectin on colon carcinogenesis.